

# Investigation on the electromagnetic radiation emitted by sub-GeV electrons in a bent crystal

L. Bandiera, E. Bagli, G. Germogli, V. Guidi\*, A. Mazzolari  
*INFN Sezione di Ferrara & Dipartimento di Fisica e Scienze della Terra,  
Università degli Studi di Ferrara Via Saragat 1, 44122 Ferrara, Italy*

H. Backe, W. Lauth  
*Institut für Kernphysik der Universität Mainz, Fachbereich Physik,  
Mathematik und Informatik, D – 55099 Mainz, Germany*

A. Berra, D. Lietti, M. Prest  
*Università degli Studi dell'Insubria, via Valleggio 11, 22100 Como,  
Italy & INFN Sezione di Milano Bicocca, Piazza della Scienza 3, 20126 Milano, Italy*

D. De Salvador  
*INFN Laboratori Nazionali di Legnaro, viale dell'Università 2, 35020 Legnaro,  
Italy & Dipartimento di Fisica, Università Di Padova, Via Marzolo 8, 35131 Padova, Italy*

E. Vallazza  
*INFN Sezione di Trieste, Via Valerio 2, 34127 Trieste, Italy*

V. Tikhomirov  
*Research Institute for Nuclear Problems, Belarusian State University, Minsk, Belarus\**  
(Dated: June 1, 2015)

The radiation emitted by 855 MeV electrons via planar channeling and volume reflection in a 30.5  $\mu\text{m}$  thick bent Si crystal has been investigated at MAMI (MAInzer MIkrotron) accelerator. The spectral intensity resulted to be much more intense than for an equivalent amorphous material, and peaked in the MeV range in the case of channeling radiation. Differently from a straight crystal, also for an incidence angle larger than the Lindhard angle the spectral intensity remains nearly as high as for channeling. This is due to volume reflection, for which the intensity keeps high at large incidence angle over the whole angular acceptance, which is equal to the bending angle of the crystal. Monte Carlo simulations demonstrated that incoherent scattering significantly influences both radiation spectrum and intensity either for channeling or volume reflection. In the latter case, it has been shown that incoherent scattering increases the radiation intensity due to the contribution of volume-captured particles. As a consequence, the experimental spectrum becomes a mixture of channeling and pure volume reflection radiations. These results allow a better understanding of the radiation emitted by electrons subjected to coherent interactions in bent crystals within a still unexplored energy range, which is relevant for possible applications for innovative and compact X- or  $\gamma$ -ray sources.

PACS numbers: 61.85.+p, 29.27.-a

The electromagnetic radiation emitted in the interaction of electron/positron beams with crystals has been investigated for years and in some cases exploited for the production of intense electromagnetic radiation [1–4]. The main feature of this kind of radiation [5–7] is the higher intensity of hard photo-production as compared to the case of bremsstrahlung in an amorphous medium, which is described by the Bethe and Heitler formulation (BH) [8]. The enhancement of the bremsstrahlung spectrum of electrons/positrons crossing the periodic structure of a crystal, which appeared for the first time in the works of Ferretti [9], Ter-Mikaelian [10], Dyson and Uberall [11], leads to the possibility to exploit this type of radiation as a source of intense X- or  $\gamma$ -rays far harder than the photon energies achievable in magnetic undu-

lators at the same primary electron beam energy. Such effect took the name *coherent bremsstrahlung* (CB) and was experimentally proven true by Diambri-Palazzi et al. at Frascati in 1960. In 1964, Lindhard introduced the concept of coherent scattering of charged particles by the atoms of a crystal when the particle trajectory is nearly aligned with a crystal axis/plane. In such low-angle approximation, correlations between successive collisions of a particle with the atoms in the same row/plane occur [12] and one can replace the potentials of separate atoms with an average continuous potential of the crystal atomic string/plane. The atomic string/plane steers a particle away from or towards the lattice atoms, depending on the particle's charge sign. If the incident angle with respect to the crystallographic axes/planes is

smaller than  $\theta_L = \sqrt{2U_0/pv}$ , charged particles can be confined inside the axial/planar potential well,  $U_0$  being the potential well depth,  $p$  and  $v$  the particle momentum and velocity, respectively. This effect is called *channeling* and, even though it was discovered by computer simulations in 1963 [13], only the introduction of the continuous potential by Lindhard allowed a simple description and understanding of such phenomenon. Channeled particles oscillate during their motion inside the planar/axial potential well, leading to a peculiar process of radiation emission by electrons or positrons, thereby called channeling radiation (CR) [14].

Even though CB and CR in straight crystals have been deeply investigated, new opportunities for intense production of e.m. radiation are offered by the usage of bent crystals. In particular, the radiation accompanying volume reflection (VR) in curved crystals is promising for relevant applications, spanning from a  $\gamma$ - or a positron source to a crystal-based collimation in future electron/positron colliders [15–17]. VR consists in the deflection of over-barrier particles to a direction opposite to that of the crystal bending by an angle of the order of  $\theta_L$  [18]. Because the particles that suffer VR are found in over-barrier states, they cannot be affected by dechanneling, leading to higher deflection efficiencies than for the channeling case, for either positive [19, 20] or negative [21] particles. The lower dependence of the radiation accompanying VR on the particle charge sign makes this radiation very attractive for applications in electron accelerators, which are much more common, less expensive and often offer the best performance in terms of emittance than currently available positron accelerators. Another advantage of the radiation accompanying VR is the large and adjustable angular acceptance for its generation. Indeed, the angular acceptance is practically equal to the bending angle of the crystal and considerably exceeds those for CB and CR in a straight crystal [22]. This feature would open up new possibilities for its application with the usage of relatively poor emittance electron beams.

The few existing studies on VR radiation have been done with hundreds-GeV beams [16, 22–25]. In those experiments, *mm-long* bent crystals were used, while, since the dechanneling length for GeV electrons is of the order of 20  $\mu\text{m}$  [26], bent crystals with a thickness comparable to such a length are needed to steer sub-GeV electron beams. Only very recently such a possibility was demonstrated for either channeling or VR [27, 28]. These results opened up a new challenge for e.m. radiation generation in bent crystals within the energy range accessible by many electron accelerators worldwide. In fact, there is some wealth of data concerning the radiation emitted by electrons in straight crystals in the sub-GeV/GeV energy range, while no experimental data on radiation in bent crystals does exist in the literature, but only theoretical expectations [29, 30].

In this Letter, we report on a study about the radiation generated by 855 MeV electrons through coherent interaction with a bent crystal. The electron beam was accelerated at MAInzer MIkrotron [31]. Such study aims at investigating the influence of the curvature on the radiation emitted by electrons in a bent crystal and thereby the radiation accompanying VR within an energy range interesting for an X- or  $\gamma$ -source.

The experimental setup of [26] was upgraded with a microstrip Si detector with a spatial resolution of 10  $\mu\text{m}$  [32] in order to reconstruct the beam profile after interaction with the crystal [27]. The photons emitted by the electrons inside the crystal were separated by the charged beam through a bending magnet and after 8.627 m arrived at a 10" x 10" NaI scintillator detector. An aperture of 40 mm diameter in the lead shield surrounding the detector permitted the collection of a portion of the emitted photons, resulting in a collimator aperture of 4.63 mrad, i.e., equal to  $\sim 7.8$  times the  $1/\gamma$  angle, for collection of most of the emitted photons. More details on the experimental setup can be found in [33]. Following the idea presented in [34], a Si crystal was bent through the quasimosaic effect [35] along its (111) planes. Crystal thickness along the beam was  $(30.5 \pm 0.5) \mu\text{m}$  and its bending radius was 33.5 mm, being approximately 23 times the critical radius for channeling at this energy ( $R_c = 1.5$  mm) [27, 36]. Beam divergence was about 30  $\mu\text{rad}$  of standard deviation along the direction transverse to the (111) planes, i.e., much less than  $\theta_L$ , which is about 220  $\mu\text{rad}$  at 855 MeV.

Before measuring the radiation spectra, the particle dynamics has been investigated in order to ensure the proper experimental conditions for channeling and VR, while probing at the same time the steering capability of the crystal [27]. Fig. 1(a) represents the distribution of the beam particles after the interaction with the crystal vs. the crystal-to-beam orientation. The labels (1)-(6) on the figure highlight different regions of interest. In regions (1) and (6) the crystal is not aligned with the beam, so that neither channeling nor VR occur. Region (2) corresponds to planar channeling, while region (3) is populated by dechanneled particles. Dechanneling consists in the kick out of a particle from a channel, due to incoherent scattering suffered by the particle on crystal nuclei and electrons. After a dechanneling event, the transverse energy of a channeled electron becomes higher than the planar potential barrier, i.e., a particle passes from an *under-* to an *over-*barrier state. Incoherent scattering may also cause rechanneling of previously dechanneled particles [27]. Regions (4) and (5) correspond to VR and volume capture (VC) [37], respectively. Those phenomena manifest themselves as the crystal is oriented in such a way that, even in the case of an incidence angle larger than  $\theta_L$ , the beam trajectory becomes tangent to the bent atomic planes in the crystal bulk. Under such conditions, most of the particles undergo VR [18], while

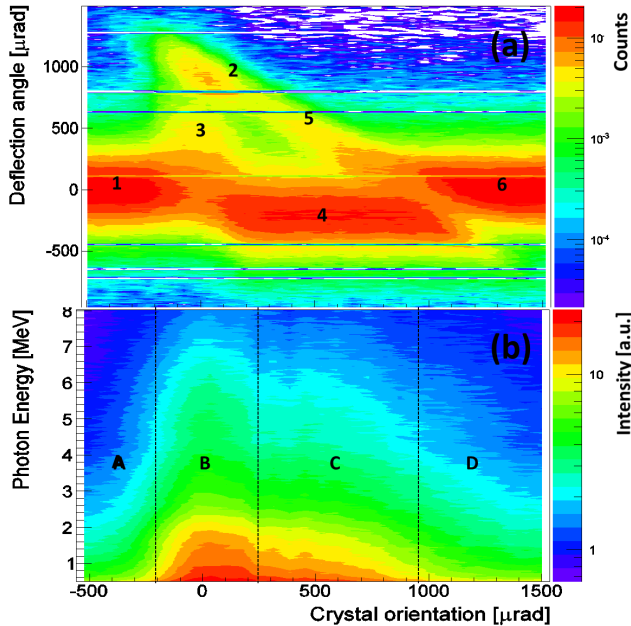


FIG. 1. (a) Experimental deflected beam distribution vs. the incoming angle with respect to the bent (111) planes. Different regions of interest are labeled by different numbers: (1) and (6) crystal for not-alignment case, (2) for channeling, (3) for dechanneling, (4) for VR, and (5) for VC. This is a reproduction of Fig. 2a in Ref. [27]. (b) Experimental radiation spectrum vs. the incoming angle with respect to the bent (111) planes. Regions (A) and (D) correspond to the nonchanneling case, (B) is for channeling and (C) for VR.

a fraction of the beam is captured into the channeling regime (VC) due to incoherent scattering [19].

In order to measure the radiation spectrum, a calibration of the NaI detector was performed by using the natural radioactive isotopes  $^{40}\text{K}$  (1.461 MeV) and  $^{208}\text{Tl}/^{228}\text{Th}$  (2.6146 MeV). The energy scale has been selected in the region of interest for CR. The experimental radiation spectrum after interaction with the crystal as a function of the crystal-to-beam angle is shown in Fig. 1 (b). Regions (A) and (D) correspond to the nonchanneling case, (B) is for channeling and (C) for VR. Region (B) also includes the contribution of the radiation emitted by the particles that were dechanneled during their motions. Similarly, the contribution of volume-captured particles is also included in region (C). As expected the radiation intensity is stronger for CR (B) than for the misaligned case (A and D). Moreover, the intensity in region C of Fig. 1(b) is still higher than for the misaligned case within the whole angular acceptance of VR, corresponding to  $\sim 900 \mu\text{rad}$ . Fig. 1 (b) differs considerably if compared to the case of a straight crystal. Indeed, in the latter case the radiation intensity falls off very rapidly out of the channeling region, which is as large as  $2\theta_L = 440 \mu\text{rad}$ , passing from CR to CB radiation.

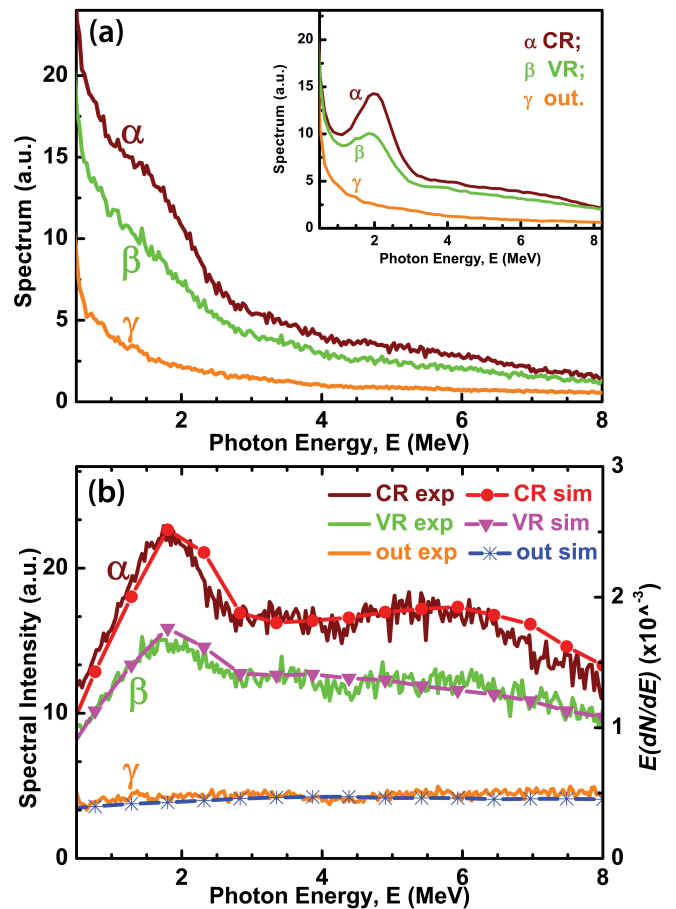


FIG. 2. (a) Experimental radiation spectra (solid lines) for the cases of channeling ( $\theta_{in} = 0 \mu\text{rad}$ ,  $\alpha$ ), VR ( $\theta_{in} = 493 \mu\text{rad}$ ,  $\beta$ ) and far from (111) bent planes ( $\theta_{in} = 8726 \mu\text{rad}$ ,  $\gamma$ ). Beam-off background has been subtracted. The experimental scale has been chosen from 0.5 MeV to 8 MeV to select the region of interest for CR. Inset of Fig. 2(a): experimental radiation spectra (solid lines) for the cases of channeling ( $\alpha$ ), VR ( $\beta$ ) and far from (111) bent planes ( $\gamma$ ), obtained with a smaller collimator aperture (4 mm instead of 40 mm) as compared to Fig. 2a. (b) Experimental (left-scale) and simulated (right-scale) radiation spectral intensities obtained by multiplying the experimental spectra in Fig. 2(a) by the photon energy,  $E$ , for the three cases. The photon emission intensity for one electron,  $E(dN/dE)$ , has been obtained averaging over one thousand of trajectories.

Fig. 2 (a) shows the experimental spectra for the radiation emitted as the crystal was oriented in channeling ( $\alpha$ -curve), in the middle of VR region ( $\beta$ -curve) and far from the alignment condition with bent planes ( $\gamma$ -curve, recorded at an angle of  $\theta_{in} = 8726 \mu\text{rad}$  from channeling). The experimental scale has been chosen from 0.5 MeV to 8 MeV to select the region of interest for CR. The depicted spectra are unprocessed, i.e., the deconvolution from the detector response function has not been performed. Nevertheless, the effect of the finite resolution would influence mostly the lower part of the spectra

(< 0.5 MeV), far from the CR region [26]. The intensities for both CR ( $\alpha$ ) and the radiation accompanying VR ( $\beta$ ) are stronger than for the case far from channeling ( $\gamma$ ). The experimental spectra represent the total radiation collected by the NaI detector, which is proportional to the number of photons by unit of time and energy. For the sake of better comparison with the spectra usually displayed in the literature, Fig. 2 (b) highlights the spectral intensities obtained by multiplying the experimental spectra in Fig. 2 (a) by the photon energy,  $E$ . The spectral intensity of CR peaks for photon energies close to 1.8 MeV, which also appears in the case of VR, though less intense. Since many applications in nuclear physics or medicine do require nearly-monochromatic MeV photon beams [38, 39], we repeated the measurements for CR and radiation accompanying VR with a smaller collimator aperture (4 mm instead of 40 mm) to reject the contribution of the soft radiation emitted at large angles. The experimental results show the possibility to pass from the total un-peaked spectra of Fig. 2 (a) to the peaked ones displayed in the inset.

For the interpretation of experimentally recorded patterns, we performed Monte Carlo simulations with the code DYNECHARM++ [40] and its extension including RADCHARM++ [30] for radiation computation. The DYNECHARM++ code takes into account the real particle trajectories, and thereby the contribution of incoherent scattering, too. The algorithm to compute the radiation emission probability implemented in RADCHARM++ is based on direct integration of the general formula of Baier and Katkov for the electromagnetic radiation generated by charged particles in an external field [41].

The simulated spectral intensities  $E(dN/dE)$  vs.  $E$ ,  $dN/dE$  being the photon emission probability for each electron, for channeling (circles), VR (down triangles) and misaligned cases (stars), are displayed in Fig. 2, showing a good agreement with the experiments in both shape and amplitude.

In Ref. [27], it was shown that incoherent scattering plays a crucial role in the electron dynamics under coherent interaction with the bent  $30.5 \mu\text{m}$  Si crystal, highlighting the contribution of dechanneling/rechanneling to the deflection efficiency. Fig. 3 shows the simulated spectral intensities for CR (circles and squares) and VR (down and up triangles) by taking (circles and down-triangles) or not taking (squares and up-triangles) into account the incoherent scattering. For comparison, the simulated Bethe-Heitler value is also shown (diamonds). As expected, CR is suppressed by the contribution of incoherent scattering [42]. Indeed, since CR is generated by the oscillatory motion of particles inside the planar potential well, the scattering events that cause particle dechanneling lead to a reduction of CR intensity. On the contrary, when the crystal is oriented in VR condition, the incoherent scattering enhances the emitted radiation.

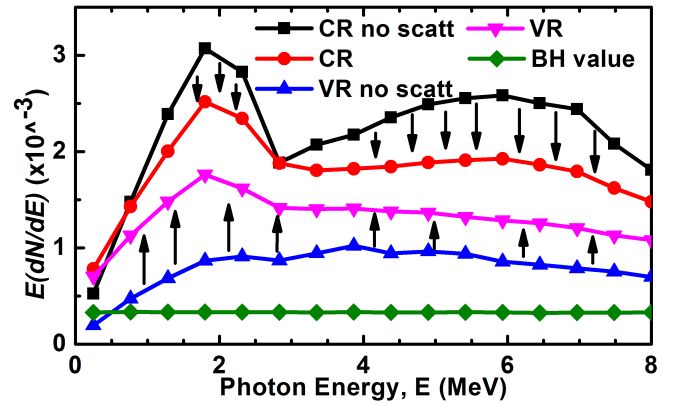


FIG. 3. Simulated spectral intensity  $E(dN/dE)$  vs. photon energy  $E$  for channeling (circles and squares) and VR (down and up triangles) by taking (circles and down-triangles) or not taking (squares and up-triangles) into account the incoherent scattering. For comparison, the simulated Bethe-Heitler value is also shown (diamonds). The arrows directed downwards underline the intensity decrease for CR caused by the incoherent scattering. The arrows directed upwards underline the intensity increase, due to incoherent scattering, for the radiation accompanying VR.

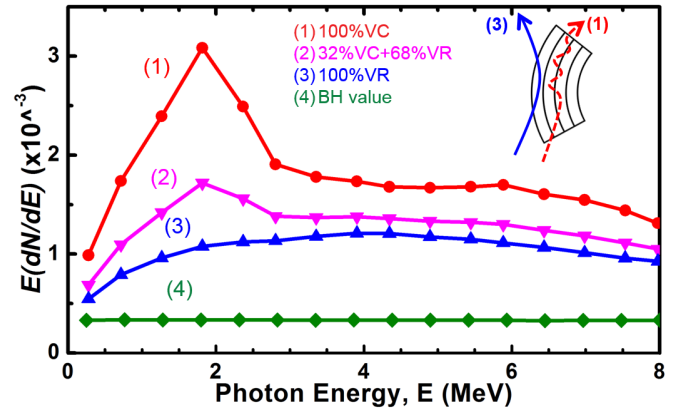


FIG. 4. Simulated spectral intensity  $E(dN/dE)$  vs. photon energy  $E$  for; (1) volume-captured particles, (3) volume-reflected particles and (2) for the total radiation accompanying VR, including both the contributions (1) and (3). (4) The simulated Bethe-Heitler value is also shown. Inset: Schematic representations of a captured (1) and a reflected (3) electron trajectories in a region close to the bent (111) planes.

This observation has never been reported before and is ascribed to the contribution of volume-captured particles. More precisely, after capture into the channel, such particles undergo a dynamics typical of channeled particles, resulting in similar radiation processes as for CR. For a better understanding, we investigated through simulations the dynamics of those particles that contributed to the spectral intensity in Fig. 3 down triangles. These particles impinged onto the crystal at  $493 \mu\text{rad}$  from bent (111) planes, thereby they are either reflected or captured

as shown in Fig. 1(a). It turned out that 68% of the initial population undergo VR, while the remaining 32% is being captured into planar channeling as a result of VC.

Fig. 4 highlights the cases if all the particles were ideally volume-reflected (curve 3) or volume-captured (curve 1). The VR spectral intensity (curve 3) does not show any peak due to the change in the angle between particle trajectory and crystal planes as the particle approaches the reflection point (see trajectory 3 in the inset in Fig. 4) [22–24, 41], while the VC spectral intensity (curve 1) is more intense than for VR and shows the typical spectrum for CR (Fig. 3 circles). Indeed, a captured electron is found in channeling condition under about half of its motion (see trajectory 1 in the inset in Fig. 4). Curve 2 represents the total contribution to radiation accompanying VR in real cases, in which the weighted VC (curve 1) and VR (curve 3) contributions are included.

The radiation accompanying VR is comparable in intensity to the radiation in a straight crystal, i.e., it is a sort of intermediate case between CR and CB, and exhibits some important features. First of all, the radiation accompanying VR possesses an adjustable and broader angular acceptance than CR and CB, which can be used for high-intensity radiation generation with poor emittance beams. Second, the steering efficiency of VR is less sensitive to crystalline defects as compared to channeling [43], opening up a way to the usage of higher-Z materials such as W, which usually cannot be grown with the same perfection as a Si crystal, while being more suitable for radiation generation [43, 44]. Finally, the process of photon generation under VR conditions comes together with particle steering, thereby the combination of these two physical effects can be useful in some practical applications. As an example, it was proposed to use VR and the accompanying radiation in a possible crystal-based collimation scheme for future electron-positron colliders [15]. The choice of VR instead of channeling can be preferable for some applications due to its higher deflection efficiency and wider angular acceptance.

In summary, the possibility to exploit bent crystals to generate hard and very intense electromagnetic radiation has been experimentally demonstrated and well reproduced by simulations. It has also been demonstrated that CR and the radiation accompanying VR are much more intense than for an amorphous material. In particular, it was shown how the radiation accompanying VR naturally combines the radiation emitted by pure volume-reflected particles with that emitted as a result of VC. The contribution of VC radiation renders the radiation accompanying VR similar to that for CR in intensity, but its angular acceptance is wider than for channeling. The combination of these features provides interesting prospects for applications of the e.m. radiation generated in bent crystals for the electron accelerators available worldwide.

We acknowledge the partial support of INFN under the CHANEL experiment and the European Commission

under the CUTE Project. The research leading to these results has received funding from the European Community's Seventh Framework Programme FP7/2007-2013 under Grant Agreement Nr. 227431. In particular, we acknowledge Dr. Gerald Klug and Dr. Eugen Eurich from Disco Europe (Munich, Germany) for their support in crystal manufacturing, Mr. Andrea Persiani and Mr. Claudio Manfredi of Perman (Loiano, Italy) for their support in crystal holders manufacturing, Gilles Frequet from Fogale Nanotech for precise measurement of crystal thickness by means of a T-MAP IR interferometer.

---

\* [guidi@fe.infn.it](mailto:guidi@fe.infn.it)

- [1] J.D. Kellie *et al.*, Nuclear Instruments and Methods in Physics Research Section A: Accelerators, Spectrometers, Detectors and Associated Equipment **545**, 164 (2005).
- [2] D. Lohmann, J. Peise, J. Ahrens, I. Anthony, H.-J. Arends, R. Beck, R. Crawford, A. Hüniger, K. Kaiser, J. Kellie, *et al.*, Nuclear Instruments and Methods in Physics Research Section A: Accelerators, Spectrometers, Detectors and Associated Equipment **343**, 494 (1994).
- [3] N. Shul'ga, International Journal of Modern Physics A **25**, 9 (2010).
- [4] T. Koenig and U. Oelfke, Physics in Medicine and Biology **55**, 1327 (2010).
- [5] M. L. Ter-Mikaelian, *High-energy Electromagnetic Processes in Condensed Media* (Wiley, New York, 1972).
- [6] V. Baier, V. Katkov, and V. Strakhovenko, *Electromagnetic Processes at High Energies in Oriented Single Crystals* (World Scientific, Singapore, 1998).
- [7] A. Akhiezer and N. Shulga, *High-energy electrodynamics in matter* (Gordon & Breach, New York, 1996).
- [8] H. Bethe, W. Heitler, Proc. Roy. Soc. **146**, 83 (1934).
- [9] B. Ferretti, Nuovo Cim. **7**, 118 (1950).
- [10] M. Ter-Mikaelian, Zh. Exp. Teor. Fiz. **25**, 296 (1953).
- [11] H. Uberall, Phys. Rev. **103**, 1055 (1956).
- [12] J. Lindhard, Danske Vid. Selsk. Mat. Fys. Medd. **34**, 14 (1965).
- [13] M. T. Robinson and O. S. Oen, Applied Physics Letters **2**, 30 (1963).
- [14] M. Kumakhov, Physics Letters A **57**, 17 (1976).
- [15] A. Seryi, Nuclear Instruments and Methods in Physics Research Section A: Accelerators, Spectrometers, Detectors and Associated Equipment **623**, 23 (2010).
- [16] L. Bandiera *et al.*, Phys. Rev. Lett. **111**, 255502 (2013).
- [17] L. Bandiera *et al.*, Journal of Physics: Conference Series **517**, 012043 (2014).
- [18] A. Taratin and S. Vorobiev, Phys. Lett. A **119**, 425 (1987).
- [19] W. Scandale *et al.*, Phys. Rev. Lett. **98**, 154801 (2007).
- [20] E. Bagli *et al.*, The European Physical Journal C **74**, 1 (2014).
- [21] W. Scandale *et al.*, Phys. Lett. B **681**, 233 (2009).
- [22] Yu. A. Chesnokov *et al.*, Journal of Instrumentation **3**, P02005 (2008).
- [23] W. Scandale, *et al.*, Phys. Rev. A **79**, 012903 (2009).
- [24] D. Lietti *et al.*, Nuclear Instruments and Methods in Physics Research Section B: Beam Interactions with Materials and Atoms **283**, 84 (2012).

- [25] L. Bandiera et al., Nuclear Instruments and Methods in Physics Research Section B: Beam Interactions with Materials and Atoms **309**, 135 (2013).
- [26] H. Backe, P. Kunz, W. Lauth, and A. Rueda, Nuclear Instruments and Methods in Physics Research Section B: Beam Interactions with Materials and Atoms **266**, 3835 (2008).
- [27] A. Mazzolari et al., Phys. Rev. Lett. **112**, 135503 (2014).
- [28] U. Wienands, T. Markiewicz, J. Nelson, R. Noble, J. Turner, U. Uggerhøj, T. Wistisen, E. Bagli, L. Bandiera, G. Germogli, *et al.*, Physical review letters **114**, 074801 (2015).
- [29] R. G. Polozkov, V. K. Ivanov, G. B. Sushko, A. V. Korol, and A. V. Solovyov, The European Physical Journal D **68**, 1 (2014).
- [30] L. Bandiera, E. Bagli, V. Guidi, and V. V. Tikhomirov, Nuclear Instruments and Methods in Physics Research Section B: Beam Interactions with Materials and Atoms (2015).
- [31] A. Jankowiak, Eur. Phys. J. A **28**, 149 (2006).
- [32] D. Lietti, A. Berra, M. Prest, and E. Vallazza, Nuclear Instruments and Methods in Physics Research Section A: Accelerators, Spectrometers, Detectors and Associated Equipment **729**, 527 (2013).
- [33] D. Lietti, H. Backe, E. Bagli, L. Bandiera, A. Berra, S. Carturan, D. De Salvador, G. Germogli, V. Guidi, W. Lauth, *et al.*, Review of Scientific Instruments **86**, 045102 (2015).
- [34] V. Guidi *et al.*, J. Phys. D **42**, 182005 (2009).
- [35] Y. Ivanov, A. Petrunin, and V. Skorobogatov, Journal of Experimental and Theoretical Phys. Lett. **81**, 99 (2005).
- [36] G. Germogli, A. Mazzolari, L. Bandiera, E. Bagli, and V. Guidi, Nuclear Instruments and Methods in Physics Research Section B: Beam Interactions with Materials and Atoms (2015).
- [37] Yu.A. Chesnokov, N.A. Galyaev, V.I. Kotov, S.V. Tsarik, V.N. Zapolsky, Nuclear Instruments & Methods in Physics Research Section B-Beam Interactions with Materials and Atoms **69**, 247 (1992).
- [38] H. R. Weller, M. W. Ahmed, H. Gao, W. Tornow, Y. K. Wu, M. Gai, and R. Miskimen, Progress in Particle and Nuclear Physics **62**, 257 (2009).
- [39] D. Habs, T. Tajima, and V. Zamfir, Nuclear Physics News **21**, 23 (2011).
- [40] E. Bagli and V. Guidi, Nuclear Instruments and Methods in Physics Research Section B: Beam Interactions with Materials and Atoms **309**, 124 (2013).
- [41] V. Guidi, L. Bandiera and V. Tikhomirov, Phys. Rev. A **86**, 042903 (2012).
- [42] O. Bogdanov and S. Dabagov, in *Journal of Physics: Conference Series*, Vol. 357 (IOP Publishing, 2012) p. 012029.
- [43] E. Bagli et al., Phys. Rev. Lett. **110**, 175502 (2013).
- [44] C. Gary, R. Pantell, M. Özcan, M. Piestrup, and D. Boyers, Journal of applied physics **70**, 2995 (1991).